strongly supports the assumption of the ligand substitution of eq 8 as the rate-determining step in the present case.

The kinetic parameters for ligand substitution in $Au(NH_3)_4^{3+}$ (cf. Table III) shows that the faster the reaction, the smaller the enthalpy of activation. Thus, the kinetic discrimination between incoming ligands for the substrate $Au(NH_3)_4^{3+}$ is mainly an enthalpy effect. The entropy changes are expected to be negative for associative activation. This is the case for water as entering ligand in $Au(NH_3)_4^{3+}$ (cf. Table III). For the halides, the negative contribution to ΔS^* from the formation of the transition state is counteracted by changes in solvation due to partial charge neutralization. As expected, this latter effect is less important for iodide than for chloride. Those observations further support the identification of the substitution reaction of eq 8 as rate-determining for the redox process.

(iii) The third possibility is a direct reduction of the tetraammine complex as a result of an attack by iodide directly on coordinated ammonia and concomitant elimination of INH_3^+. This is in agreement both with the rate law of eq 5 and with the ionic strength dependence but does not seem very likely in view of the free energy relationship of Figure 2 and the other observations in support of mechanism ii discussed above.

Reaction 3. For the reaction of *trans*-$Au(NH_3)_2Cl_2^+$ and *trans*-$Au(NH_3)_2Br_2^+$ with iodide, the present experiments give no direct indication as to whether the rate-determining step is a direct reduction by iodide (eq 12) followed by the reaction of eq

$$trans\text{-}Au(NH_3)_2X_2^+ + I^- \rightarrow X^- + Au(NH_3)_2^+ + XI \quad (12)$$

11 or a substitution of chloride or bromide, respectively, by iodide (eq 13), followed by rapid trans substitution[28] and/or reduction.

$$trans\text{-}Au(NH_3)_2X_2^+ + I^- \rightarrow trans\text{-}Au(NH_3)_2XI^+ + X^- \quad (13)$$

A comparison of the rate constants determined for the reaction between *trans*-$Au(NH_3)_2X_2^+$ and iodide with those for ligand substitution reactions of some related gold(III) complexes (cf. Table III) might help to classify those reactions. A comparison of rate constants for a large number of ligand substitution reactions of various gold(III) complexes has shown that the discrimination between various incoming ligands increases with increasing positive charge on the gold(III) complex,[7] e.g. $Au(NH_3)_4^{3+}$ discriminates better between various incoming ligands than does $AuBr_4^-$. A similar trend should be expected when substitution of ammonia in $Au(NH_3)_4^{3+}$ is compared with substitution of bromide in *trans*-$Au(NH_3)_2Br_2^+$. An inspection of the rate constants given in Table III shows that substitution of ammonia in $Au(NH_3)_4^{3+}$ with iodide is 4×10^3 times faster than with chloride. For *trans*-$Au(NH_3)_2Br_2^+$, on the other hand, the rate constant for reaction with I^- is at least 3×10^4 times larger than the rate constant for the substitution of bromide with chloride. Thus, reaction with iodide is more than 10 times *faster* than expected for substitution of bromide with iodide. This seems to indicate that the *trans*-$Au(NH_3)_2Br_2^+$/iodide reaction is a direct reduction, in which a noncoordinated iodide reduces the complex via one of the bromide ligands of the complex without any initial substitution.

trans-$Au(NH_3)_2Cl_2^+$ is also expected to discriminate between entering ligands to a smaller extent than $Au(NH_3)_4^{3+}$, when substitution of a chloride in *trans*-$Au(NH_3)_2Cl_2^+$ is compared with substitution of ammonia in $Au(NH_3)_4^{3+}$. The values in Table III show that the ratio between the rate constants for NH_3/Br^- and NH_3/I^- substitution in $Au(NH_3)_4^{3+}$ is 440, whereas for *trans*-$Au(NH_3)_2Cl_2^+$ the ratio between the rate constants for Cl^-/Br^- substitution and for reaction with iodide is 130. This lower ratio is fully compatible with a Cl^-/I^- ligand substitution as rate-determining, when *trans*-$Au(NH_3)_2Cl_2^+$ reacts with iodide. There is also the possibility that this reaction represents a borderline case in which the observed overall change is a mixture of parallel substitution and direct reduction and that the observed rate constants and activation parameters are composite quantities. This might explain the opposite trend of ΔH^* and ΔS^* for reaction of *trans*-$Au(NH_3)_2Cl_2^+$ with bromide and iodide compared to the corresponding reactions of $Au(NH_3)_4^{3+}$, but on the other hand, this alternative seems less probable since the temperature dependence agrees with Arrhenius' equation for a single reaction over a fairly large interval of temperature.

Acknowledgment. Thanks are due to Eva Bredenfeldt and Bodil Øby for experimental assistance, to one of the reviewers for several valuable comments, and to the Danish and Swedish Natural Science Research Councils for financial support.

Registry No. $Au(NH_3)_4^{3+}$, 43739-93-1; *trans*-$Au(NH_3)_2I_2^+$, 104090-03-1; *trans*-$Au(NH_3)_2Br_2^+$, 70148-53-7; I^-, 20461-54-5.

Contribution from the Department of Chemistry, University of Houston, University Park, Houston, Texas 77004

Manganese(0) Radicals and the Reduction of Cationic Carbonyl Complexes: Selectivity in the Ligand Dissociation from 19-Electron Species

D. J. Kuchynka, C. Amatore,[1] and J. K. Kochi*

Received May 9, 1986

Products and stoichiometry for the cathodic reduction of the series of carbonylmanganese(I) cations $Mn(CO)_5L^+$, where L = CO, MeCN, pyridine, and various phosphines, derive from 1-electron transfer to generate the 19-electron radicals $Mn(CO)_5L^\bullet$ as reactive intermediates. The CO derivative $Mn(CO)_6^+$ affords mainly the anionic $Mn(CO)_5^-$ by the facile ligand dissociation of $Mn(CO)_6^\bullet$ to the 17-electron radical $Mn(CO)_5^\bullet$ followed by reduction. The acetonitrile and pyridine derivatives $Mn(CO)_5NCMe^+$ and $Mn(CO)_5py^+$ produce high yields of the dimer $Mn_2(CO)_{10}$ by an unusual and highly selective heterolytic coupling of $Mn(CO)_5^-$ and the reactant cation. Structural factors involved in the conversion of 19-electron radicals to their 17-electron counterparts are examined in the reduction of the graded series of phosphine derivatives $Mn(CO)_5P^+$, where P = triaryl- and trialkylphosphines. The formation of the hydridomanganese complexes $HMn(CO)_4P$ is ascribed to hydrogen atom transfer to the 19-electron radicals $Mn(CO)_5P^\bullet$ followed by extrusion of CO. The lability of carbonylmanganese radicals is underscored by rapid ligand substitution to afford the bis(phosphine) byproduct $HMn(CO)_3P_2$.

Introduction

Increased experimental evidence is accruing for the participation of paramagnetic species with an odd number of valence electrons as key, reactive intermediates in a variety of reactions of metal carbonyls.[2,3] For purposes of further discussion, we designate such transient intermediates as carbonylmetal radicals.[4] As such, from a diamagnetic 18-electron metal carbonyl there are two types of radicals possible, viz., the electron-supersaturated 19-electron species and the electron-deficient 17-electron species. These correspond to anion radicals and cation radicals if they are gen-

(1) Present address: Laboratoire de Chimie, Ecole Normale Superieure, Paris 75231 Cedex 05, France.
(2) Brown, T. L. *Ann. N. Y. Acad. Sci.* **1980**, *80*, 333.
(3) Kochi, J. K. *J. Organomet. Chem.* **1986**, *300*, 139.
(4) See: Kochi, J. K. *Organometallic Mechanisms and Catalysis*; Academic: New York, 1978; Chapter 3.

0020-1669/86/1325-4087$01.50/0

Table I. Electroreduction of Carbonylmanganese(I) Cations[a]

$Mn(CO)_5L^{+}$[b]			amt of $Mn(CO)_5^-$,	amt of $Mn_2(CO)_{10}$,	amt of $Mn_2(CO)_8P_2$,	amt of $HMn(CO)_4P$,	amt of $HMn(CO)_3P_2$,	material balance,
L	amt, mmol	n[c]	mmol (%)	mmol (%)	mmol (%)	mmol (%)	mmol (%)	%
CO[d]	0.39	1.4	0.24 (61)	0.012 (6)				67[e]
MeCN	0.18	1.3	0.068 (38)	0.039 (43)				81
py	0.16	1.1	0.024 (15)	0.049 (61)				76
PPh_3	0.17	1.3	0.063 (37)	0	0.038 (45)	0.023 (14)	0.0052 (3)	99
$(p\text{-MeOPh})_3P$	0.11	1.3	0.038 (35)	0	0.030 (56)	0.0077 (7)	0.0016 (2)	100
$(o\text{-MeOPh})_3P$	0.13	1.4	0.078 (60)	0.0054 (8)	0.0055 (8)	0	0	76
$p\text{-Tol}_3P$	0.15	1.3	0.065 (43)	0	0.026 (35)	0.016 (10)	0.017 (11)	99
Et_2PhP	0.15	1.3	0.040 (27)	0	0.038 (52)	0.019 (13)	0.016 (11)	103
$EtPh_2P$	0.14	1.1	0.024 (18)	0	0.040 (58)	0.016 (12)	0	88
Et_3P	0.13	1.1	0.015 (12)	0	0.033 (51)	0.040 (30)	0	93
$MePh_2P$	0.16	1.2	0.044 (28)	0	0.048 (60)	0.0096 (6)	0.012 (8)	102
Me_2PhP	0.14	1.1	0.016 (11)	0	0.041 (58)	0.036 (26)	trace	95

[a] In THF containing 0.3 M TBAP at 25 °C unless stated otherwise. [b] As BF_4^- or PF_6^- salt. [c] Electron uptake relative to $Mn(CO)_5L^+$. [d] In acetonitrile containing 0.2 M TBAP. [e] Black deposit on cathode and 1 equiv of CO evolved.

erated by electron transfer to and from a neutral metal carbonyl precursor. Likewise, a cationic metal carbonyl upon reduction affords a neutral 19-electron radical, which will generate either a neutral or cationic 17-electron radical by loss of an uncharged or anionic ligand, respectively.

Cognizance must be taken of at least four important factors in delineating the reactivities of carbonylmetal radicals. First, the behavior of 17- and 19-electron species must be distinguished from each other and compared to that of their diamagnetic counterparts. Furthermore, ion radicals are to be differentiated from uncharged radicals owing to large differences in solvation and (ion) pairing effects, especially in nonpolar solvents relevant to metal carbonyl chemistry.[5] Finally, the relationship to the more conventional and well-known homolytic reactions of organic free radicals[6] must be established.

In order to compare the reactivity of 19- and 17-electron radicals in relationship to their 18-electron precursor, we examined the follow-up reactions attendant upon the reduction of the series of carbonylmanganese cations $(OC)_5MnL^+$, where L = phosphines, acetonitrile, pyridine, and carbon monoxide. In this study the pertinent species are (a) the 18-electron cation $(OC)_5MnL^+$, (b) the 19-electron radical $(OC)_5MnL^{\bullet}$ formed upon reduction, and (c) the 17-electron radicals $(OC)_4MnL^{\bullet}$ or $(OC)_5Mn^{\bullet}$ resulting from the loss of either a carbon monoxide or a ligand L (acetonitrile, pyridine or phosphine), respectively.

Results

For purposes of our study, we arbitrarily classified the carbonylmanganese cations $(OC)_5MnL^+$ into three groups: I, L = carbon monoxide; II, **L** = the nitrogen-centered ligands acetonitrile and pyridine; III, L = phosphorus(III) ligands consisting of a series of aryl- and alkylphosphines with different base strengths and steric properties. Each of the carbonylmanganese cations was prepared as a pure crystalline solid that was readily characterized by its distinctive carbonyl stretching bands (ν_{CO}) in the IR spectrum.[7,8] Thus, the parent hexacarbonylmanganese(I) cation (I) was obtained as colorless crystals (ν_{CO} = 2096.7 cm^{-1}) from sodium pentacarbonylmanganate and ethyl chloroformate followed by cleavage with boron trifluoride.[8] The acetonitrile derivative $(OC)_5Mn(NCMe)^+$ (IIa) was obtained as colorless crystals (ν_{CO} = 2162, 2074, 2050 cm^{-1}) from the oxidative cleavage of dimanganese decacarbonyl in acetonitrile with nitrosonium hexafluorophosphate.[7] It was converted to the yellow pyridine derivative IIb (ν_{CO} = 2155, 2101, 2046 cm^{-1}) by treating IIa with 4 equiv of pyridine in refluxing chloroform for 15 h:

$$(OC)_5Mn(NCMe)^+ + py \xrightarrow[CHCl_3]{} (OC)_5Mn(py)^+ + MeCN \quad (1)$$

The series of phosphine analogues III ($\nu_{CO} \cong$ 2140, 2090, 2050 cm^{-1}) were also prepared from the acetonitrile derivative by a slow ligand substitution carried out in the dark, as described in the Experimental Section:[7,9]

$$(OC)_5Mn(NCMe)^+ + PPh_3 \rightarrow (OC)_5MnPPh_3^+ + MeCN \quad (2)$$

I. Reduction Products of Carbonylmanganese(I) Cations. The hexacarbonylmanganese cation (I) was cathodically reduced by passing a constant current of 3 mA through an acetonitrile solution (5×10^{-3} M) containing 0.2 M tetra-*n*-butylammonium perchlorate. The electroreduction was accompanied by the vigorous evolution of 1.0 ± 0.1 mol of carbon monoxide for each mole of reactant. The total charge passed through the solution corresponded to ~1.4 C/mol of I. The current was interrupted when the electrode potential increased from −1.15 to −1.55 V vs. SCE, which signaled the end of the electrolysis of $Mn(CO)_6^+$. The same coulometric results were obtained when the reduction was carried out potentiostatically at −1.20 V. In both cases, the products were characterized as pentacarbonylmanganate, $Mn(CO)_5^-$ (61%), and the dimer $Mn_2(CO)_{10}$ (6%) in Table I. The analysis of the catholyte was carried out by quantitative IR spectroscopy using the distinctive carbonyl bands ν_{CO} for $Mn(CO)_5^-$ at 1865 and 1900 cm^{-1} and for $Mn_2(CO)_{10}$ at 2045, 2012, and 1983 cm^{-1} by comparison with those of authentic samples.[10-12] Both of these manganese carbonyls accounted for an overall material balance of only 67% according to the stoichiometry in eq 3. Part of the

$$Mn(CO)_6^+ \xrightarrow{[+e^-]} [Mn(CO)_5^- + Mn_2(CO)_{10}] + CO \quad (3)$$

deficit could be attributed to a black solid that coated the electrode surface. It was insoluble in common organic solvents such as dichloromethane, tetrahydrofuran, and acetone but readily dissolved in concentrated nitric acid to afford a colorless solution that was not characterized further.

The reduction of the carbonylmanganese cations IIa and IIb containing nitrogen-centered ligands in tetrahydrofuran proceeded in much the same manner as for the parent I.[13] However, the stoichiometry in eq 4 required that 1 mol of acetonitrile rather

$$(OC)_5MnNCMe^+ \xrightarrow{[+e^-]} [Mn(CO)_5^- + Mn_2(CO)_{10}] + MeCN \quad (4)$$

than carbon monoxide be liberated. The product mixture consisted of relatively less $Mn(CO)_5^-$ (38%) and more of the dimeric

(5) For example, see: Kao, S. C.; Darensbourg, M. Y.; Schenk, W. *Organometallics* **1984**, *3*, 871 and related papers.
(6) Kochi, J. K., Ed. *Free Radicals*; Wiley: New York, 1973; Vols. 1 and 2.
(7) Darensbourg, D. J.; Darensbourg, M. Y. *Inorg. Chem.* **1975**, *14*, 1779.
(8) Beach, N. A.; Gray, H. B. *J. Am. Chem. Soc.* **1968**, *90*, 5713.
(9) See also: Reimann, R. H.; Singleton, E. *J. Chem. Soc., Dalton Trans.* **1976**, 2109.
(10) King, R. B.; Stone, F. G. A. *Inorg. Synth.* **1963**, *3*, 198.
(11) Wrighton, M. S.; Faltynek, R. A. *J. Am. Chem. Soc.* **1978**, *100*, 2701.
(12) Brimm, E. O.; Lynch, M. A.; Sesny, W. J. *J. Am. Chem. Soc.* **1954**, *76*, 3831.
(13) Note that the sparing solubility of $Mn(CO)_6^+BF_4^-$ in THF necessitated the use of acetonitrile.

Table II. Cathodic Peak Potentials E_p^c of Carbonylmanganese(I) Cations: Solvent Dependence[a]

$Mn(CO)_5L^+X^-$	tetrahydrofuran	acetonitrile
$Mn(CO)_6^+BF_4^-$	*b*	−1.27
$Mn(CO)_5py^+BF_4^-$	−0.81	−1.12
$Mn(CO)_5NCMe^+PF_6^-$	−0.84	−1.19
$Mn(CO)_5PPh_3^+PF_6^-$	−1.05	−1.29
$Mn(CO)_5[(p\text{-}MeOPh)_3P]^+PF_6^-$	−1.21	−1.37
$Mn(CO)_5[(o\text{-}MeOPh)_3P]^+PF_6^-$	−1.18	−1.45
$Mn(CO)_5[(p\text{-}Tol)_3P]^+PF_6^-$	−1.19	−1.34
$Mn(CO)_5(Ph_2EtP)^+PF_6^-$	−1.24	−1.39
$Mn(CO)_5(PhEt_2P)^+PF_6^-$	−1.32	−1.55
$Mn(CO)_5Et_3P^+PF_6^-$	−1.36	−1.67
$Mn(CO)_5(Ph_2MeP)^+PF_6^-$	−1.16	−1.41
$Mn(CO)_5(PhMe_2P)^+PF_6^-$	−1.34	−1.54

[a] Cyclic voltammetry in THF with 0.3 M TBAP and in acetonitrile with 0.1 M TEAP at 20 °C; initial concentration of $Mn(CO)_5L^+X^-$ = 5×10^{-3} M. E_p^c values are in V vs. SCE. [b] Insoluble.

$Mn_2(CO)_{10}$ (43%), together with a minor unidentified component (see Experimental Section). No electrode pollution was observed with II.

The series of phosphine derivatives III of $Mn(CO)_6^+$ generally consumed ~1.3 electrons in electroreduction to yield a rather complex mixture of products that accounted for essentially all of the $(CO)_5Mn(phosphine)^+$ charged. Thus in addition to $Mn(CO)_5^-$, three new products appeared. The bis(phosphine) $Mn_2(CO)_8(phosphine)_2$ generally replaced $Mn_2(CO)_{10}$ as the dimeric product, except with the sterically hindered tris(*o*-methoxyphenyl)phosphine. The formation of the hydridomanganese complexes $HMn(CO)_4(phosphine)$ and $HMn(CO)_3(phosphine)_2$ were unique to III. Both hydrides were readily characterized in the ^1H NMR spectrum by the appearance of distinctive hydride resonances at δ ~−7 and confirmed by comparison of the IR spectra with those of authentic samples (see Experimental Section).[14,15] Accordingly, the partial stoichiometry for the reduction of the carbonylmanganese cations $(OC)_5Mn(phosphine)^+$ can be represented as

$$(OC)_5Mn(phosphine)^+ \xrightarrow{[+e^-]} \begin{cases} Mn(CO)_5^- & (5) \\ Mn_2(CO)_8P_2 & (6) \\ HMn(CO)_4P,\ HMn(CO)_3P_2 & (7) \end{cases}$$

where P represents triaryl- and trialkylphosphines. Indeed, the relative amounts of each type of carbonylmanganese product depended strongly on the phosphine structure, as listed in Table I.

II. Transient Electrochemistry of Carbonylmanganese(I) Cations. In order to trace the origin of the various types of products obtained from the reduction of carbonylmanganese cations, we used transient electrochemical techniques, particularly cyclic voltammetry and double-step chronoamperometry, to probe for reactive intermediates.

A. The cyclic voltammograms of the three classes of monosubstituted carbonylmanganese cations I–III share in common a single irreversible cathodic wave upon an initial negative-potential scan. Calibration of the cathodic peak current with a ferrocene standard indicated that these waves corresponded to an uptake of 1.1–1.5 C/mol of the cationic carbonylmanganese reactant,[16] which agrees with the coulometric results in Table I.

The CV peak potentials E_p^c of the cathodic waves were strongly dependent on the solvent, the nature of the ligand L, and the CV sweep rate. Thus the values of E_p^c determined in acetonitrile were generally displaced 20–30 mV to more negative potentials relative to those obtained in tetrahydrofuran (see Table II). Furthermore, the cathodic waves for the cations with nitrogen ligands occurred at the least negative potentials, and the CV waves of the phosphine derivatives were the most negative. The trend in E_p^c generally paralleled the σ-donor properties of L. Thus the peak potentials became more negative in the order L = py < MeCN < CO < phosphines.

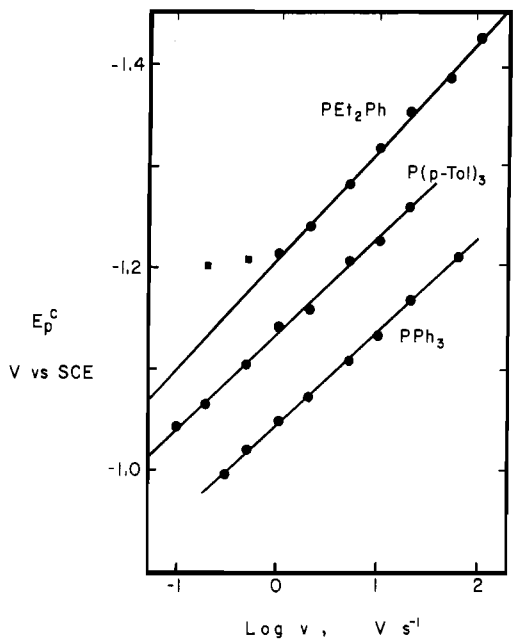

Figure 1. Variation in the cathodic CV peak potential E_p^c with scan rate (v) of selected carbonylmanganese cations $Mn(CO)_5L^+$ (from top to bottom): L = PEt_2Ph (α = 0.28, r = 0.999); L = $P(p\text{-}CH_3Ph)_3$ (α = 0.32, r = 0.998); L = PPh_3 (α = 0.33, r = 0.999). α = transfer coefficient, and r = correlation coefficient. The data denoted by boxes (■) were excluded from the linear regression analysis.

Table III. Anodic Peak Potentials E_p^a of Carbonylmanganese(I) Anions $Mn(CO)_4P^-$ and $Mn(CO)_5^-$: Solvent Dependence[a]

	acetonitrile		tetrahydrofuran	
P	$Mn(CO)_4P^-$	$Mn(CO)_5^-$	$Mn(CO)_4P^-$	$Mn(CO)_5^-$
CO		−0.12	*b*	
py		−0.12		−0.05
MeCN		−0.13		−0.04
PPh_3	−0.50	−0.11	−0.52	−0.05
$P(p\text{-}MeOPh)_3$	−0.52	−0.12	−0.50	−0.04
$P(o\text{-}MeOPh)_3$		−0.12		−0.04
$P(p\text{-}Tol)_3$	−0.53	−0.13	−0.51	−0.04
$PEtPh_2$	−0.54	−0.12	−0.52	−0.04
PEt_2Ph	−0.57	−0.12	−0.53	−0.03
PEt_3	−0.58	−0.11	−0.60	−0.04
$PMePh_2$	−0.53	−0.12	−0.55	−0.03
PMe_2Ph	−0.55	−0.12	−0.56	−0.04

[a] From cyclic voltammetry of $Mn(CO)_5L^+$ in acetonitrile with 0.1 M TEAP and in THF with 0.3 M TBAP at 20 °C; initial concentration of $Mn(CO)_5L^+$ = 5×10^{-3} M. E_p^a values are in V vs. SCE. L = P (phosphines). [b] Insoluble.

The dependence of E_p^c on the CV sweep rate (log v) is shown in Figure 1 for the carbonylmanganese cations of some representative phosphine ligands. A linear correlation is observed at reasonable sweep rates with slopes in the range of 70–85 mV/unit of log v. A close inspection of Figure 1 indicates that the slopes vary with L, e.g., α = 0.33 for PPh_3 but 0.28 for PEt_2Ph.

It is interesting to note that the anodic peak potential E_p^a for the phosphine-substituted carbonylmanganate anion $Mn(CO)_4P^-$ is strikingly insensitive to structural variations in P (see Table III). Furthermore, the values of E_p^a are the same in acetonitrile and tetrahydrofuran within experimental scatter, especially in comparison with the corresponding changes in E_p^a of $Mn(CO)_5^-$ with the same solvent variation. The apparent discrepancy may be due to a compensation of solvent and electronic effects in the oxidation

(14) (a) Gladysz, J. A.; Tam, W.; Williams, G. M.; Johnson, D. L.; Parker, D. W. *Inorg. Chem.* **1979**, *18*, 1163. (b) Ruszczyk, R. J.; Bih-Lian, H.; Atwood, J. D. *J. Organomet. Chem.* **1986**, *299*, 205.
(15) Ugo, R.; Bonati, F. *J. Organomet. Chem.* **1967**, *8*, 189.
(16) The cathodic peak currents and potentials were calibrated relative to a known amount of ferrocene as an internal standard. See: Gagne, R. R.; Koval, C. A.; Lisensky, G. C. *Inorg. Chem.* **1980**, *19*, 2854.

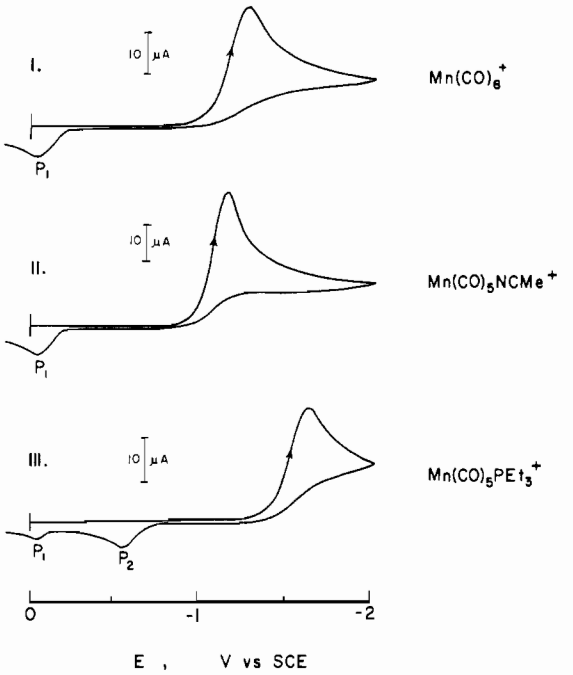

Figure 2. Initial negative-scan cyclic voltammograms of carbonylmanganese cations $Mn(CO)_5L^+$ where L = CO (I), MeCN (IIa), and PEt_3 (III) in acetonitrile containing 0.1 M TBAP with a scan rate v = 500 mV s^{-1} at 20 °C.

of $Mn(CO)_4P^-$. Nonetheless, the contrasting results in Tables II and III do emphasize the different sensitivities of $Mn(CO)_5P^+$ and $Mn(CO)_4P^-$ during reduction and oxidation, respectively, as a result of the changes in phosphine structures.

The cyclic voltammograms of the carbonylmanganese cations I–III are distinguished by their behavior on the return *positive* scan. This difference is exemplified in Figure 2 for L = CO (I), MeCN (II), and PEt_3 (III) by the appearance of either a single or a pair of anodic waves P_1 and P_2. The anodic CV wave P_1 is readily assigned to the oxidation of pentacarbonylmanganate (IV); i.e.

$$\underset{\text{IV}}{Mn(CO)_5^-} \xrightarrow{[-e^-]} Mn(CO)_5^{\bullet} \qquad (8)$$

by comparison with the anodic behavior of the authentic salt $Mn(CO)_5^-Na^+$.[10] Moreover, the anodic wave P_2 is assigned to the mono(phosphine) analogue V by comparison with the CV behavior of $Mn(CO)_4P^-Na^+$ (where P = PMe_2Ph and PPh_3);[11] e.g.

$$\underset{\text{V}}{Mn(CO)_4PMe_2Ph^-} \xrightarrow{[-e^-]} Mn(CO)_4PMe_2Ph^{\bullet} \qquad (9)$$

The coproduction of pentacarbonylmanganate (IV) and the phosphine derivative V in Figure 2 is akin to that observed when the initial negative-scan cyclic voltammogram of $Mn(CO)_5PPh_3^+$ is carried out to the limit of the solvent "wall" (i.e., −3.1 V). In addition to the anodic waves P_1 and P_2, Figure 3 shows the presence of a cathodic wave R_2. The minor peak R_1 is attributed to the presence of small amounts of the dimeric $Mn_2(CO)_8(PPh_3)_2$ by comparison with that of an authentic sample.[7] The major cathodic peak R_2 coincides with that of the hydridomanganese complex $HMn(CO)_4PPh_3$ prepared independently.[14] (Note that the enhanced cathodic peak of $HMn(CO)_4PPh_3$ is also partly due to its proximity to the potential at which the background discharge occurred.) Thus, the CV data reveal that the primary products arising from the reduction of $Mn(CO)_5P^+$ are the hydridomanganese complex $HMn(CO)_4P$ and the two anions $Mn(CO)_5^-$ and $Mn(CO)_4P^-$.

Thus the products observed in the CV experiment differ from those obtained by bulk electrolysis in two important ways: (a) the anion $Mn(CO)_4P^-$ is prominent in the cyclic voltammogram

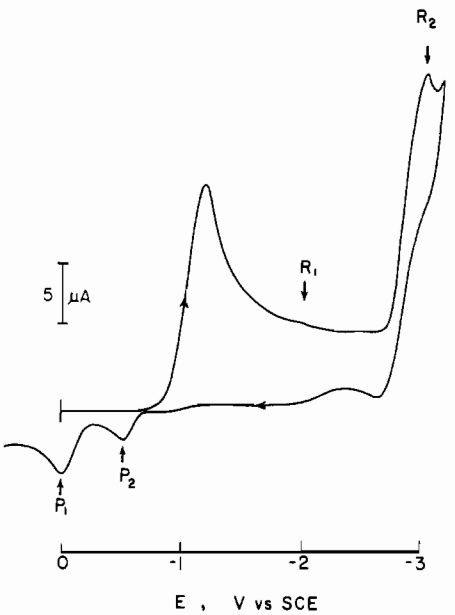

Figure 3. Initial negative-scan cyclic voltammogram of 5 × 10^{-3} M $Mn(CO)_5PPh_3^+PF_6^-$ in THF containing 0.3 M TBAP (v = 500 mV s^{-1} at 20 °C), illustrating the formation of $Mn_2(CO)_8(PPh_3)_2$, $HMn(CO)_4PPh_3$, and the anions $Mn(CO)_5^-$ and $Mn(CO)_4PPh_3^-$.

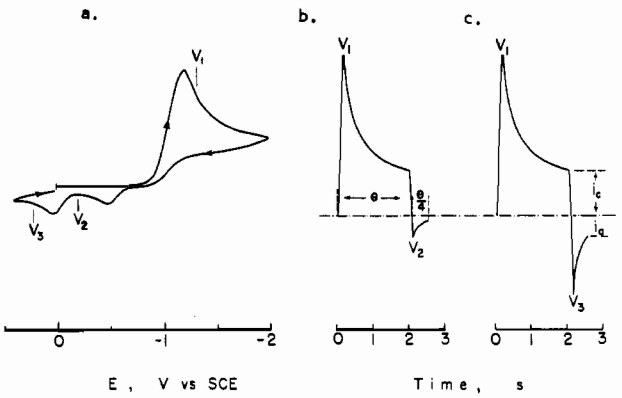

Figure 4. Double-step chronoamperometry of $Mn(CO)_5[(p\text{-}MeOPh)_3P]^+PF_6^-$ in THF containing 0.3 M TBAP: (a) cyclic voltammogram at 400 mV s^{-1} showing the location of V_1 = −1.32 V, V_2 = −0.2 V, and V_3 = 0.2 V; (b) potential jump from V_1 to V_2; (c) potential jump from V_1 to V_3. Parts b and c both have θ = 2 s.

(see the anodic wave P_2 in Figure 2), whereas it is absent in bulk electrolysis (see Table I) and (b) the dimeric $Mn_2(CO)_8P_2$ is an important constituent of bulk electrolysis (column 6, Table I) whereas only traces are observed in the cyclic voltammogram (see Figure 3). The difference is doubtlessly due to kinetic factors arising from the divergent time scales of the two electrochemical methods. Thus both methods should afford the same product distribution if the species generated at the electrode were stable within the time scale of the bulk electrolysis (ca. 0.5–1 h). However, cyclic voltammetry samples the microelectrolysis within the diffusion layer (which extends 10–30 μm from the electrode), and only those species generated within this thin annulus are readily analyzed during the same potential sweep, i.e., a few seconds after birth. Thus a detailed analysis of the CV behavior should provide insight into the reactivity of transient species. As applied to the carbonylmanganese species pertinent to this study, we focus on the formation and chemical behavior of the two anions $Mn(CO)_5^-$ and $Mn(CO)_4P^-$, the transient concentrations of which are provided by a potential-jump method.[17]

(17) For example, double-step chronoamperometry minimizes problems associated with diffusion. Thus the diminished anodic peak currents in Figure 2 are partly due to loss from diffusion that occurs prior to the reverse scan.

Table IV. Normalized Current Ratios of the Anodic CV Peak Currents from the Reduction of $Mn(CO)_5P^+$ [a]

P	R_1	R_2	r [b]	log r
PPh_3	0.056 ± 0.006	0.43 ± 0.03	6.68	0.82
$(p\text{-Tol})_3P$	0.10 ± 0.01	0.49 ± 0.01	3.90	0.58
$(p\text{-MeOPh})_3P$	0.18 ± 0.01	0.47 ± 0.02	1.61	0.21
$(o\text{-MeOPh})_3P$	0.009 ± 0.001	0.44 ± 0.02	47.9	1.7
Ph_2EtP	0.093 ± 0.02	0.38 ± 0.03	3.08	0.49
$PhEt_2P$	0.21 ± 0.02	0.34 ± 0.03	0.62	−0.21
Ph_2MeP	0.083 ± 0.008	0.34 ± 0.03	3.10	0.49
$PhMe_2P$	0.17 ± 0.01	0.29 ± 0.02	0.70	−0.15
Et_3P	[c]	[c]	0.29 [d]	−0.54

[a] From solutions of $Mn(CO)_5P^+$ in THF containing 0.3 M TBAP. For measurement of R_1 and R_2, see text and Experimental Section. [b] $r = R_2/R_1 - 1$. [c] Did not yield current ratios independent of θ. [d] For determination, see Experimental Section.

B. Double-step chronoamperometry was used to determine the relative concentrations of $Mn(CO)_5^-$ and $Mn(CO)_4P^-$ in the following manner. Using the cyclic voltammogram of the carbonylmanganese cation $Mn(CO)_5[(p\text{-}MeOC_6H_4)_3P]^+$ as an example in Figure 4a we initially set the pulse (θ) to a potential V_1 that was 100 mV past $E_p^c = -1.21$ V vs. SCE. At the end of the interval θ, the potential was jumped to a new value ($V_2 = -0.2$ V) where $Mn(CO)_4P^-$ could be oxidized without interference from $Mn(CO)_5^-$ (i.e., between anodic waves P_2 and P_1) for a period of $\theta/4$ s. The ratio R_1 of the anodic and cathodic currents i_a and i_c, respectively, was determined according to Figure 4c. In a second experiment, the same cathodic pulse was again performed at V_1, but the anodic pulse was adjusted to a different value ($V_3 = 0.2$ V) at which both $Mn(CO)_4P^-$ and $Mn(CO)_5^-$ were oxidized to yield the composite current ratio R_2 (see Figure 4c). The fraction of the anions is given by $[Mn(CO)_5^-]/[Mn(CO)_4P^-] = R_2/R_1 - 1$, as described in the Experimental Section.[18] The transient (relative) concentrations of the various carbonylmanganese anions obtained from the reduction of the cationic $Mn(CO)_5P^+$ are given in Table IV. Such a conversion corresponds to an overall 2-electron change; i.e.

$$Mn(CO)_5P^+ \xrightarrow{[+2e^-]} \begin{cases} Mn(CO)_5^- + P & (10) \\ Mn(CO)_4P^- + CO & (11) \end{cases}$$

III. Coupling of Carbonylmanganese Ions. Formation of Manganese–Manganese Dimers. The formation of significant amounts of the dimeric $Mn_2(CO)_{10}$ and $Mn_2(CO)_8P_2$ in bulk electrolysis but not in cyclic voltammetry suggests that it may arise via a rather slow thermal process stemming from a transient intermediate (vide supra). Such an intermediate could be the anion $Mn(CO)_4P^-$ owing to its absence in bulk electrolysis (Table I) but its appearance in cyclic voltammetry (Figure 3). Indeed, the separate treatment of $Mn(CO)_4PPh_3^-$ with its cationic precursor $Mn(CO)_5PPh_3^+$ under the same conditions of the electrolysis led to the dimer in essentially quantitative yields within 15 min (see Table V):

$$Mn(CO)_4PPh_3^-Na^+ + Mn(CO)_5PPh_3^+BF_4^- \rightarrow Mn_2(CO)_8(PPh_3)_2 + CO + Na^+BF_4^- \quad (12)$$

The absence of unsymmetrical dimers among the products of electroreduction provides additional support for the cross-coupling process. However, it leaves open the question as to whether the more traditional route to dimanganese carbonyls, namely via the dimerization of the radicals $Mn(CO)_5^\bullet$ and $Mn(CO)_4P^\bullet$,[19,20] is a viable process in this system. These 17-electron radicals were generated by the electrochemical oxidation of the carbonylmanganese anions. The initial positive-scan cyclic voltammogram of $Mn(CO)_4PPh_3^-$ in Figure 5 shows the irreversible, 1-electron anodic wave with $E_p^a = -0.5$ V in tetrahydrofuran. The appearance of the CV wave of the dimeric $Mn_2(CO)_8(PPh_3)_2$ is confirmed by comparison with that of an authentic sample. Judging from the magnitude of this anodic peak, we conclude that it is formed in close to quantitative yield on the CV time scale; i.e.

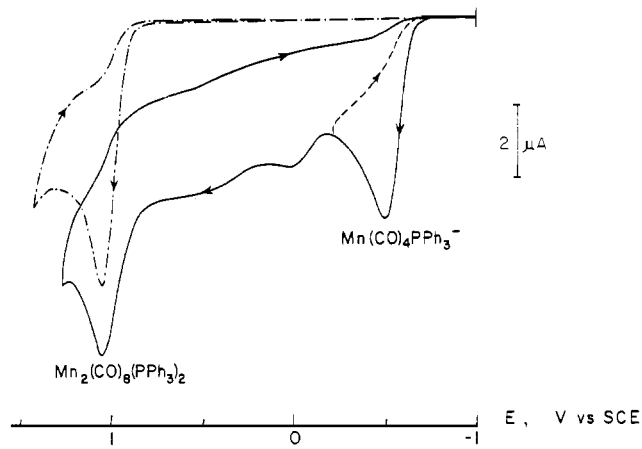

Figure 5. Initial positive-scan cyclic voltammogram (—) of 5×10^{-3} M $Mn(CO)_4PPh_3^-Na^+$ in THF with 0.3 M TBAP ($v = 500$ mV s^{-1} at 20 °C) showing the formation of $Mn_2(CO)_8(PPh_3)_2$ in near-quantitative yields. The cyclic voltammogram of 5×10^{-3} M $Mn_2(CO)_8(PPh_3)_2$ under the same conditions is shown (-·-) for comparison.

$$Mn(CO)_4PPh_3^- \xrightarrow{[-e^-]} Mn(CO)_4PPh_3^\bullet \xrightarrow{fast} {}^1/_2Mn_2(CO)_8(PPh_3)_2 \quad (13)$$

Discussion

The combined use of bulk electrolytic and transient electrochemical techniques provides the means to generate and examine the 19-electron radicals ($Mn(CO)_5L^\bullet$) VI and their associated 17-electron counterparts VII ($Mn(CO)_5^\bullet$ and $Mn(CO)_4L^\bullet$) from the related series of carbonylmanganese cations $Mn(CO)_5L^+$ (I–III).

I. Formation of the 19-Electron Radical VI. The reductions of $Mn(CO)_5L^+$ feature a single cathodic wave in the cyclic voltammetry of all three classes of cations, I–III. The cathodic peak potentials E_p^c of the irreversible waves in Table II are strongly dependent on the σ-donor properties of the ligand L. The dependence of E_p^c on the CV scan rate (log v) in Figure 1 shows that the reduction is affected by the heterogenous kinetics of the initial electron transfer; i.e.

$$Mn(CO)_5L^+ \xrightarrow{[+e^-]} \underset{VI}{Mn(CO)_5L^\bullet} \quad (14)$$

The slopes in Figure 1 correspond to transfer coefficients α of 0.3–0.4, which are in good agreement with the values of α previously reported for $Mn_2(CO)_{10}$.[21] Such a result indicates that E_p^c depends on both the driving force (E°) and the rate (k_s) of the electron transfer;[22,23] i.e.

$$E_p^c = E^\circ + \frac{RT}{\alpha F} \ln k_s - \frac{RT}{2\alpha F} \ln v + \text{constant} \quad (15)$$

(18) Note that the total anodic currents relative to the cathodic current were always less than the theoretical value of 0.146. (Actually 0.146 refers to $R = i(2\theta)/i(\theta)$, and $i(5\theta/4)/i(\theta) = 0.553$, which is to be compared with R_2 in Table IV.) This indicates that the anions $Mn(CO)_5^-$ and $Mn(CO)_4P^-$ constituted only a fraction of the reduction products (vide infra).

(19) (a) Hughey, J. L.; Anderson, C. P.; Meyer, T. J. *J. Organomet. Chem.* **1977**, *125*, C49. (b) Wegmann, R. W.; Olsen, R. J.; Gard, D. R.; Faulkner, L. R.; Brown, T. L. *J. Am. Chem. Soc.* **1981**, *103*, 6089.

(20) (a) Walker, H. W.; Herrick, R. S.; Olsen, R. J.; Brown, T. L. *Inorg. Chem.* **1984**, *23*, 3748 and references therein on $Mn(CO)_4P^\bullet$ radical dimerization. (b) The rate constant for the dimerization of $Mn(CO)_4P^\bullet$ is 2 orders of magnitude smaller than the dimerization of $Mn(CO)_5^\bullet$.

(21) Lemoine, P.; Giraudeau, A.; Gross, M. *Electrochim. Acta* **1976**, *21*, 1.

Table V. Heterolytic Coupling of Carbonylmanganese Anions and Cations[a]

entry no.	anion	cation	time[b]	products (yield, %)[c]
1	$Mn(CO)_5^-Na^+$	$Mn(CO)_5NCMe^+PF_6^-$	<15 min	$Mn_2(CO)_{10}$ (100)
2	$Mn(CO)_5^-Na^+$	$Mn(CO)_5py^+BF_4^-$	<15 min	$Mn_2(CO)_{10}$ (100)
3	$Mn(CO)_5^-Na^+$	$Mn(CO)_6^+BF_4^-$	24 h[d]	no reacn
4	$Mn(CO)_5^-Na^+$	$Mn(CO)_5PEt_3^+PF_6^-$		no reacn
5	$Mn(CO)_5^-Na^+$	$Mn(CO)_5PAn_3^+PF_6^-$[e]	>4	$Mn_2(CO)_{10}$ (15)
6	$Mn(CO)_4PPh_3^-Na^+$	$Mn(CO)_5PPh_3^+BF_4^-$	<15 min	$Mn_2(CO)_8(PPh_3)_2$ (100)

[a] In THF containing 0.3 M TBAP, unless specified otherwise; initial concentration of both ions 3×10^{-3} M. [b] Estimate of time required for reaction. [c] Formed within 30 min. [d] Carried out in MeCN with 0.2 M TBAP. See Experimental Section. [e] $PAn_3 = P(o\text{-}MeOC_6H_4)_3$.

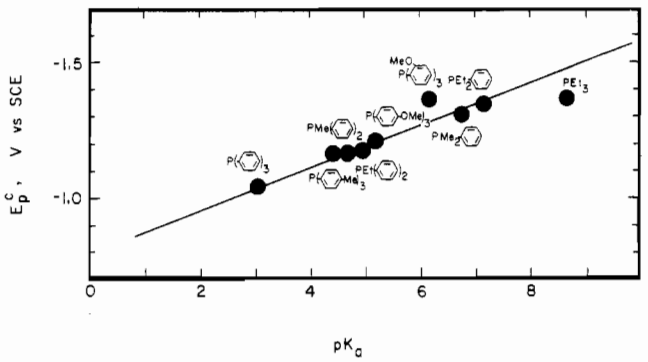

Figure 6. Correlation of the cathodic peak potentials E_p^c of 5×10^{-3} $Mn(CO)_5P^+$ (P as labeled) in THF containing 0.3 M TBAP (v = 700 mV s^{-1} at 20 °C) with the pK_a value of the phosphine (see text).

Although we could not measure $E°$ under our experimental conditions,[24] it is likely that the CV wave is under both thermodynamic and kinetic control.[25]

The behavior of phosphine derivatives of the carbonylmanganese cations $Mn(CO)_5P^+$ is particularly illustrative since these ligands form a graded series of donors that can be evaluated by the pK_a values of the protonated forms.[26] The relationship between E_p^c and pK_a in Figure 6 underscores the importance of electron accession to the manganese center for reduction in eq 14.[29,30] Such a linear correlation reflects the changes induced by a better σ-donor phosphine on the driving force ($E°$) as a result of increasing the energy of the LUMO and on the activation barrier log k_s as a result of an increased electron density in the cation.[31] Let us now focus on how the 19-electron carbonylmanganese radical VI is converted to the products listed in Table I.[32]

II. Products and Stoichiometry of the Reduction of Carbonylmanganese Cations I–III. Following the initial electron transfer in eq 14, the ultimate fate of the 19-electron radical VI is reflected in the appearance of carbonylmanganese anions and dimers as well as hydridomanganese carbonyls (see Table I). The reduction of carbonylmanganese cations to the corresponding anions (Mn^-) corresponds to a consumption of 2 electrons, whereas that to the dimers (Mn_2) and hydridomanganese (HMn) involve 1 electron (vide infra and Table I). The combined yields of these products relate directly to the net electron consumption. Accordingly, the stoichiometry of the reduction can be generally represented as

$$Mn(CO)_5L^+ + (2-\beta)e^- \rightarrow \beta[(\gamma/2)Mn_2 + (1-\gamma)HMn] + (1-\beta)Mn^- \quad (16)$$

where β and γ are a pair of constants to accord with each entry in Table I. Indeed, the variation in product distribution in Table I (i.e., $\beta \cong 0.7 \pm 0.2$) is reflected in both the coulometric measurements in bulk electrolysis and the cathodic peak currents in cyclic voltammetry. As such, we now consider how each product is formed from the 19-electron radical $Mn(CO)_5L^•$.

III. Pathways to the Manganese Hydrides, Dimers, and Anions from the 19-Electron Radical VI. The routes taken by the 19-electron radical $Mn(CO)_5L^•$ to the final products are indicated by the transient electrochemical behavior. Common to all three classes of carbonylmanganese cations I–III are the irreversible cathodic waves at ca. −1.4 V for reduction according to eq 14.

(i) From the parent cation $Mn(CO)_6^+$ (I), the subsequent formation of $Mn(CO)_5^-$ as the principal product and the coulometry in Table I accord with an overall 2-electron process, as shown in Scheme I.

Scheme I

$$Mn(CO)_6^+ \xrightarrow{[+e^-]} Mn(CO)_6^• \quad (17)$$

$$Mn(CO)_6^• \xrightarrow{[+e^-]} Mn(CO)_5^- + CO \quad (18)$$

(ii) From the nitrogen-centered derivatives $Mn(CO)_5py^+$ (IIb) and $Mn(CO)_5NCMe^+$ (IIa) the formation of $Mn(CO)_5^-$ together with the dimeric $Mn_2(CO)_{10}$ accords with the facility of the cross-coupling of the anion–cation pair, which was demonstrated in Table V, e.g. as shown in Scheme II.

Scheme II

$$Mn(CO)_5NCMe^+ \xrightarrow{[+e^-]} Mn(CO)_5NCMe^• \quad (19)$$

$$Mn(CO)_5NCMe^• \xrightarrow{[+e^-]} Mn(CO)_5^- + MeCN \quad (20)$$

$$Mn(CO)_5^- + Mn(CO)_5NCMe^+ \xrightarrow{fast} Mn_2(CO)_{10} + MeCN \quad (21)$$

(22) (a) Nadjo, L.; Saveant, J. M. *J. Electroanal. Chem. Interfacial Electrochem.* **1973**, *48*, 113. The electron-transfer coefficient is given by $\alpha = -(RT \ln (10/nF))/(\partial E_p/\partial \log v) \cong -30/(\partial E_p/\partial \log v)$ at room temperature, where $(\partial E_p/\partial \log v)$ is the slope in Figure 1 of the E_p vs. log v correlation expressed in mV. (b) Saveant, J. M.; Tessier, D. *J. Phys. Chem.* **1978**, *82*, 1723.

(23) See also: Bard, A. J.; Faulkner, L. R. In *Electrochemical Methods*; Wiley: New York, 1980.

(24) No evidence of chemical reversibility was observed up to scan rates of 100 V s^{-1}. This indicates that the half-life of the 19-electron radical $Mn(CO)_5L^•$ is less than 0.25 ms.

(25) (a) Furthermore, the latter is likely to be influenced by the rate of the follow-up reactions of the 19-electron radical.[22] (b) See also: Klingler, R. J.; Kochi, J. K. *J. Am. Chem. Soc.* **1980**, *102*, 4790.

(26) The pK_a values relate primarily to the formation of a pure σ bond (i.e., PH^+) and do not include any back-bonding contribution.[27] Strictly speaking, steric effects of L must also be considered in dealing with phosphine complexes.[28]

(27) See, e.g.: Cotton, F. A.; Wilkinson, G. *Advanced Inorganic Chemistry*, 4th ed.; Wiley: New York, 1981; p 1185ff.

(28) Zizelman, P. M.; Amatore, C.; Kochi, J. K. *J. Am. Chem. Soc.* **1984**, *106*, 3771.

(29) The linear correlation in Figure 6 is given by $E_p^c = 0.07pK_a - 0.85$ with a correlation coefficient of 0.97 when the CV peak potentials are given in V vs. SCE at 700 mV s^{-1}. Owing to differences in the transfer coefficient, (vide supra), the slope is dependent on the sweep rate.

(30) For a similar behavior in oxidation, see ref 25b and: Klingler, R. J.; Kochi, J. K. *J. Am. Chem. Soc.* **1981**, *103*, 5839.

(31) Compare: Andrieux, C. P.; Blocman, C.; Dumas-Bouchiat, J. M.; Saveant, J. M. *J. Am. Chem. Soc.* **1980**, *102*, 3806. Falsig, M.; Lund, H.; Nadjo, L.; Saveant, J. M. *Nouv. J. Chim.* **1980**, *4*, 445.

(32) The 19-electron radical VI, however transient,[24] is considered to be an intermediate in the electroreduction of carbonylmetal cations. However, the chemical irreversibility of the initial cathodic CV wave precludes a proof. The alternative dissociative electron attachment does not adequately explain the relationship in Figure 6. A similar situation has been discussed in connection with the anodic oxidation of organometals.[30] For related 19-electron intermediates, see also: Meyer, T. J.; Caspar, J. V. *Chem. Rev.* **1985**, *85*, 187. Stiegman, A. E.; Tyler, D. R. *Coord. Chem. Rev.* **1985**, *63*, 217.

(iii) From the phosphine derivatives $Mn(CO)_5P^+$ (III) the formation of $Mn(CO)_5^-$, $Mn_2(CO)_8P_2$, and $HMn(CO)_4P$ accords with the foregoing steps together with the incursion of a hydrogen transfer, as shown in Scheme III.

Scheme III

$$Mn(CO)_5P^+ \xrightarrow{[+e^-]} Mn(CO)_5P^\bullet \quad (22)$$

$$Mn(CO)_5P^\bullet \xrightarrow{[+e^-]} Mn(CO)_5^- + P \quad (23a)$$

$$Mn(CO)_5P^\bullet \xrightarrow{[+e^-]} Mn(CO)_4P^- + CO \quad (23b)$$

$$Mn(CO)_4P^- + Mn(CO)_5P^+ \rightarrow Mn_2(CO)_8P_2 + CO \quad (24)$$

$$Mn(CO)_5P^\bullet + SH \rightarrow HMn(CO)_4P, \text{ etc.} \quad (25)$$

According to the formulations in Schemes I–III, the reductions of the carbonylmanganese cations are differentiated by the behavior of (a) the 19-electron radical $Mn(CO)_5L^\bullet$ and (b) the associated anions $Mn(CO)_5^-$ and $Mn(CO)_4L^-$, which are delineated below.

IV. Formation of Carbonylmanganese Anions. 17-Electron Radicals VII as Intermediates. The conversion of the 19-electron radical $Mn(CO)_5L^\bullet$ to the anion III and IV in eq 17, 19, and 22 formally requires an electron accession and a ligand loss, for which there are two sequential possibilities. Thus it can proceed via a prior electron transfer to form an unstable intermediate followed by ligand loss; i.e.

$$Mn(CO)_5L^\bullet \xrightarrow{[+e^-]} Mn(CO)_5L^- \xrightarrow{-L} Mn(CO)_5^- \quad (26)$$

The overall transformation from the carbonlymanganese cation corresponds to an electrochemical EEC process. The formation of the 20-electron intermediate $Mn(CO)_5L^-$ requires the uptake of the second electron in eq 26 to occur at essentially the same (or a more positive) potential as the initial electron transfer—an unlikely possibility.[33] The alternative sequence involves prior ligand loss to produce the 17-electron radical VII followed by electron accession; i.e.

$$Mn(CO)_5L^\bullet \xrightarrow{-L} Mn(CO)_5^\bullet \xrightarrow{[+e^-]} Mn(CO)_5^- \quad (27)$$

This is a more reasonable formulation since it circumvents the hexacoordinate 20-electron intermediate. It corresponds overall to an electrochemical ECE process.[34] Owing to the irreversibility of the initial electron transfer in eq 14,[35] the EEC and ECE formulations are difficult to differentiate definitively by quantitative analysis of the transient electrochemical behavior. However, evidence has accrued in the related 19-electron bis(phosphine) radical $Mn(CO)_3(NCMe)P_2^\bullet$ that reduction to the anion $Mn(CO)_3P_2^-$ proceeds by an ECE process.[36] Proceeding from the same basis, we judge that the decomposition in eq 18 (Scheme I) of the 19-electron radical $Mn(CO)_6^\bullet$ by the ejection of carbon monoxide is immediately followed by reduction of the 17-electron radical VII; i.e.

$$Mn(CO)_6^\bullet \xrightarrow{-CO} Mn(CO)_5^\bullet \xrightarrow{fast} Mn(CO)_5^- \quad (28)$$

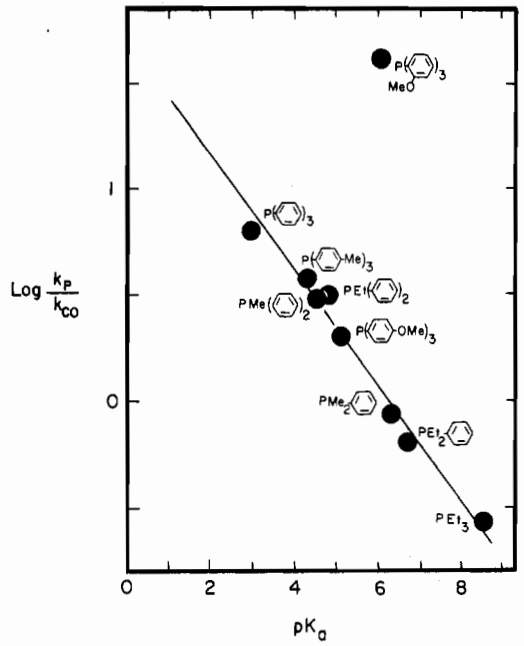

Figure 7. Competition in the loss of CO and phosphine P from the 19-electron radical $Mn(CO)_5P^\bullet$ as a function of the pK_a value of the phosphine, as described in the text.

since only small amounts of the dimer $Mn_2(CO)_{10}$ are obtained.[37]

However, the loss of carbon monoxide from the substituted radical $Mn(CO)_5NCMe^\bullet$ in eq 20 (Scheme II) is not competitive with the expulsion of acetonitrile, since $Mn_2(CO)_{10}$ was obtained as the sole dimer (see Table I) and only $Mn(CO)_5^-$ was observed in the cyclic voltammogram (see Figure 2b);[38] i.e.

$$Mn(CO)_5NCMe^\bullet \xrightarrow{-MeCN} Mn(CO)_5^\bullet \quad (29a)$$

IV

$$Mn(CO)_5NCMe^\bullet \xrightarrow{-CO} Mn(CO)_4NCMe^\bullet \quad (29b)$$

V

This selectivity is in accord with the expected difference in leaving group abilities of carbon monoxide relative to the nitrogen-centered ligands acetonitrile and pyridine.[39]

For the phosphine analogue in eq 23 (Scheme III), the results in Table IV show that there is competition between the loss of carbon monoxide and phosphine; i.e.

$$Mn(CO)_5P^\bullet \xrightarrow{-P} Mn(CO)_5^\bullet \xrightarrow{[+e^-]} IV \quad (30a)$$

$$Mn(CO)_5P^\bullet \xrightarrow{-CO} Mn(CO)_4P^\bullet \xrightarrow{[+e^-]} V \quad (30b)$$

The direct relationship between the relative rates of ligand loss (i.e., log (k_P/k_{CO})) and the pK_a value of the phosphine ligand is shown in Figure 7.[40] Such a linear correlation underscores the

(33) (a) See e.g.: Amatore, C.; Gareil, M.; Saveant, J. M. *J. Electroanal. Chem. Interfacial Electrochem.* **1983**, *147*, 1. (b) Even if both electron-transfer steps occur at or near the same potential on enthalpic grounds, a broadening of the CV wave would occur as a result of entropic differences (Ammar, F.; Saveant, J. M. *J. Electroanal. Chem. Interfacial Electrochem.* **1973**, *47*, 215).

(34) It is important to emphasize that the reductions of the 17-electron radicals to the anions III and IV are rapid, owing to large driving forces for electron transfer. Thus the 17-electron radicals are generated at the potential of the cathodic wave (see E_p^c in Table II) but undergo facile reduction at significantly more positive potentials (see E_p^a in Table III). Thus, the lifetimes of the 17-electron radicals formed under these reductive conditions are expected to be short.

(35) Indeed, the irreversibility of the cathodic CV wave is readily attributable to the rapid rate of ligand loss in eq 27.[24]

(36) (a) Narayanan, B. A.; Amatore, C.; Kochi, J. K. *Organometallics*, in press. (b) The same applies to the neutral metal carbonyls $Fe(CO)_5$ and $Cr(CO)_6$. Narayanan, B. A.; Amatore, G.; Kochi, J. K. *Organometallics* **1986**, *5*, 926.

(37) (a) Note that the cross-coupling of the anion–cation pair in this system is ineffective (see Table V). The small amounts of $Mn_2(CO)_{10}$ may arise via homolytic coupling. (b) The constancy of R_1 and R_2 with θ (see Table IV and Experimental Section) shows that the formation of Mn^- and HMn derives from a competition between reactions of identical molecularity stemming from a common intermediate. Since HMn is formed via a 1-electron process (which precludes an EEC mechanism), the same must be true for Mn^-. Thus, the ECE nature of Mn^- formation is most likely.

(38) (a) Although $Mn(CO)_4NCMe^-$ is unknown, we judge from the trend in E_p^a in Table III and for various $Cr(CO)_5L$[38b] and $CpMn(CO)_2L$[28] that E_p^a is more negative than that (−0.5 V) of $Mn(CO)_4PPh_3^-$. The absence of such an anodic wave indicates that $Mn(CO)_4NCMe^-$ is not present in significant amounts. (b) Hershberger, J. W.; Klingler, R. J.; Kochi, J. K. *J. Am. Chem. Soc.* **1982**, *104*, 3034.

(39) See the discussion in ref 28 and 38.

strong electronic influence on this competition. The steric effect on the decomposition of these radicals is minor, with the exception of the tris(*o*-methoxyphenyl)phosphine derivative (see Figure 7). However, the free ligand in this complex radical is highly encumbered, as reflected in the estimated cone angle $\theta \cong 195°$ in comparison with that (145°) of triphenylphosphine.[41] This sterically crowded radical also affords much higher yields of $Mn(CO)_5^-$ by phosphine loss relative to those for the *p*-methoxy isomer, despite its comparable property (pK_a) as a donor ligand.[42] Likewise, it is the only phosphine derivative in Table I that afforded $Mn_2(CO)_{10}$, the otherwise expected dimer $Mn_2(CO)_8[(o\text{-}MeOC_6H_4)_3P]_2$ being obtained in low yield. Since these results merely reflect the competition in eq 30, they leave open the question as to whether the phosphine structure affects ligand loss of the 19-electron radical VI in eq 30a or ligand stabilization of the 17-electron radical VII in eq 30b.[43] However, the preferential expulsion of phosphine from the 19-electron radical VI is indicated by the observation of only $Mn(CO)_5^-$ and no $Mn(CO)_4P^-$ from the sterically hindered phosphine[42] $(o\text{-}MeOC_6H_4)_3P$ in cyclic voltammetry and in bulk electrolysis. A similar penchant for enhanced dissociation of an ortho-substituted triarylphosphine has been measured in the rate-limiting phosphine loss in the reductive elimination of (triarylphosphine)organogold complexes.[44]

V. Formation of the Dimeric Dimanganese Carbonyls from Ion Pairs. The unusual pattern of dimeric manganese carbonyls produced in Table I derives from the highly selective heterolytic coupling of carbonylmanganese anions and cations; i.e.

$$Mn(CO)_4L^- + Mn(CO)_5L^+ \rightarrow Mn_2(CO)_8L_2 + CO \qquad (31)$$

The cyclic voltammograms in Figures 2 and 3 indicate that the carbonylmanganese anions $Mn(CO)_5^-$ and $Mn(CO)_4P^-$ are formed at the electrode in the midst of rather high local concentrations of their cationic precursors $Mn(CO)_5L^+$ (where L = NCMe, py, phosphine, CO, etc.). Thus the rate of the cross-coupling reaction in eq 31 will determine how much dimer is formed and how little anion survives in the bulk electrolysis. Indeed the results in Table I show that the yields of $Mn_2(CO)_{10}$ and $Mn_2(CO)_8P_2$ vary considerably with the nature of L. Accordingly, we examined the facility with which the cross-coupling occurs with various combinations of carbonylmanganese anions and cations. The strikingly high selectivities shown in Table V support the cross-coupling of anion–cation pairs as a major route to dimer formation. Thus the relative high yield of $Mn_2(CO)_{10}$ obtained from the electroreduction of $Mn(CO)_5py^+$ and $Mn(CO)_5NCMe^+$ accords with the rapid rate of the corresponding cross-coupling reaction (see entries 1 and 2 in Table V). Likewise, the limited amounts of $Mn_2(CO)_{10}$ obtained from the electroreduction of $Mn(CO)_6^+$ are consistent with the inertness of the cationic I (see entry 3 in Table V).[45]

VI. Formation of Hydridomanganese Complexes from the 19-Electron Radical VI. The production of the hydridomanganese complex $HMn(CO)_4P$ from the reduction of carbonylmanganese cations is observed principally from the phosphine derivatives $Mn(CO)_5P^+$. The results in Table I also show that minor but definite amounts of the corresponding hydrido–bis(phosphine) complex $HMn(CO)_3P_2$ are also formed. In the reduction of the analogous bis(phosphine) cations $Mn(CO)_4P_2^+$, we presented evidence of hydrogen atom transfer to the initially formed 19-electron radical VI.[36] The same formulation applied to the carbonylmanganese cation III is presented in Scheme IV, in which

Scheme IV

$$Mn(CO)_5P^+ \xrightarrow{[+e^-]} Mn(CO)_5P^\bullet \qquad (32)$$

$$Mn(CO)_5P^\bullet \xrightarrow{SH} HCOMn(CO)_4P + S^\bullet, \text{ etc.} \qquad (33)$$

$$HCOMn(CO)_4P \rightarrow HMn(CO)_4P + CO \qquad (34)$$

the solvent or supporting electrolyte can serve as the hydrogen atom donor SH.[46] Although the formyl intermediate has been observed in the bis(phosphine) complex, we expect $HCOMn(CO)_4P$ to be too transient in eq 34 for direct examination.[48] An alternative pathway for the formation of hydridomanganese complexes involves the 17-electron radical VII, as shown in Scheme V. This direct pathway is disfavored under the reductive con-

Scheme V

$$Mn(CO)_5P^+ \xrightarrow{[+e^-]} Mn(CO)_5P^\bullet \qquad (35)$$

$$Mn(CO)_5P^\bullet \rightarrow Mn(CO)_4P^\bullet + CO \qquad (36)$$

$$Mn(CO)_4P^\bullet \xrightarrow{SH} HMn(CO)_4P + S^\bullet, \text{ etc.} \qquad (37)$$

ditions prevailing in the electrolysis for the following reason. It is seen in Figure 5 that the 17-electron radical $Mn(CO)_4P^\bullet$ formed by the oxidation of the anionic $Mn(CO)_4P^-$ undergoes quantitative coupling to the dimer $Mn_2(CO)_8P_2$. Thus, any hydrogen atom transfer to $Mn(CO)_4P^\bullet$ from the same solvent–supporting electrolyte system is easily overwhelmed by rapid dimerization of the complex; i.e.

$$Mn(CO)_4P^\bullet \rightarrow {}^1/_2Mn_2(CO)_8P_2 \qquad (38a)$$

$$Mn(CO)_4P^\bullet \xrightarrow{SH} HMn(CO)_4P \qquad (38b)$$

Thus the competition in eq 38 does not occur despite the second-order kinetics, which works against dimerization. By way of contrast, when the 17-electron radical is produced under reductive conditions (from $Mn(CO)_5P^+$), the homolytic dimerization does not compete with reduction (vide supra); i.e.

$$Mn(CO)_4P^\bullet \xrightarrow{[+e^-]} Mn(CO)_4P^- \qquad (39a)$$

$$Mn(CO)_4P^\bullet \rightarrow {}^1/_2Mn_2(CO)_8P_2 \qquad (39b)$$

By taking the rate of dimerization in eq 38a and 39b to be the same, we conclude that hydrogen atom transfer to the 17-electron radical as in Scheme V does not occur in the electrolytic medium under the conditions extant in the electroreduction of carbonylmetal cations.[49]

The favored mechanism in Scheme IV also readily accommodates the formation of the bis(phosphine) hydridomanganese complex $HMn(CO)_3P_2$ as a byproduct. Thus the 17-electron radicals similar to $Mn(CO)_4P^\bullet$ are known to be highly labile.[50]

(40) The linear correlation in Figure 7 is described by $\log([Mn(CO)_5^-]/[Mn(CO)_4P^-]) = -0.26pK_a + 1.70$, with a correlation coefficient of 0.99.
(41) Tolman, C. A. *Chem. Rev.* **1977**, *77*, 313.
(42) However, for the electronic effect of an *o*-methoxy group on phenylphosphines via through-space 2p–3d overlap, see: McEwen, W. E.; Janes, A. B.; Knapczyk, J. W.; Kyllingstad, V. L.; Shiau, W.-I.; Shore, S.; Smith, J. H. *J. Am. Chem. Soc.* **1978**, *100*, 7304.
(43) Of the two possibilities, we favor the effect of phosphine on ligand loss (eq 30a) since the effect of phosphine on the stabilization of the 17-electron radical *VII* in eq 30b is likely to be minor (compare Table III). The trans effect or trans influence in these systems merits further study.
(44) Komiya, S.; Shibue, A. *Organometallics* **1985**, *4*, 684.
(45) A detailed study of anion–cation annihilation to produce dimeric manganese carbonyls will be prepared separately.
(46) For the possibility of proton transfer,[47] see the discussion in ref 36.
(47) Compare: Zotti, G.; Zecchin, S.; Pilloni, G. *J. Organomet. Chem.* **1983**, *246*, 61. M'Halla, F.; Pinson, J.; Saveant, J. M. *J. Am. Chem. Soc.* **1980**, *102*, 4120.
(48) (a) Narayanan, B. A.; Amatore, C. A.; Kochi, J. K. *Organometallics* **1984**, *3*, 802. (b) See also: Berke, H.; Huttner, G.; Scheidsteger, O.; Weiler, G. *Angew. Chem., Int. Ed. Engl.* **1984**, *23*, 735.
(49) This underscores the difference between the 19-electron $Mn(CO)_5P^\bullet$ and the 17-electron $Mn(CO)_4P^\bullet$ in their ability to effect hydrogen atom transfer in eq 33 and 36, respectively. The enhanced reactivity of $Mn(CO)_5P^\bullet$ may be attributed to the relatively high localization of spin density on the carbon atom of a bent carbonyl ligand as in the related 19-electron species $Fe(CO)_5^{\bullet-}$. See: Fairhurst, S. A.; Morton, J. R.; Preston, K. F. *J. Chem. Phys.* **1982**, *77*, 5872.

Table VI. Physical Properties of the Carbonylmanganese(I) Cations $Mn(CO)_5L$

L[a]	ν_{CO}, cm^{-1} [b]	mp, °C	anal. for C and H, % calcd	anal. for C and H, % found
MeCN	2162.3, 2074.4, 2050.2	160 dec		
py[c]	2155.0, 2100.7, 2046.4	125 dec		
PPh_3[c]	2144.0, 2073.0, 2055.0[d]	160 dec		
P(*p*-Tol)$_3$	2141.9, 2090.3, 2052.4[d]	170 dec		
P(*o*-MeOPh)$_3$	2138.0, 2087, 2049.5[d]	164 dec	45.1, 3.06	44.86, 3.12
P(*p*-MeOPh)$_3$	2140.5, 2088.6, 2051.2[d]	162 dec	45.1, 3.06	45.93, 3.52
$PEtPh_2$	2143.1, 2089.0, 2053.0	142 dec	41.2, 2.73	40.93, 2.87
PEt_2Ph	2141.6, 2088.4, 2049.7[d]	139 dec	35.6, 2.99	35.69, 3.04
PEt_3[c]	2141.6, 2083, 2049.1	143 dec[e]	33.0, 3.78	32.79, 3.88
$PMePh_2$[c]	2143.2, 2093, 2053.0[d]	173 dec[e]	44.8, 2.72	44.66, 2.77
PMe_2Ph[c]	2143.2, 2088.4, 2051.4[d]	127 dec[e]	37.2, 2.64	37.12, 2.68
CO[c]	2096.7	*f*		

[a] As the PF_6^- salt unless specified otherwise. [b] In acetonitrile unless indicated otherwise. [c] BF_4^- salt. [d] In acetone. [e] For PF_6^- salt. [f] Decomposes to $Mn_2(CO)_{10}$ on heating.

Since ligand substitution in such a radical occurs by an associative mechanism,[51] the attack of phosphine (liberated in eq 30a) in the diffusion layer would generate the 19-electron bis(phosphine) radical, as shown in Scheme VI. The bis(phosphine) radical

Scheme VI

$$Mn(CO)_4P^\cdot + P \rightarrow Mn(CO)_4P_2^\cdot \quad (40)$$

$$Mn(CO)_4P_2^\cdot \rightarrow Mn(CO)_3P_2^\cdot + CO \quad (41)$$

$Mn(CO)_4P_2^\cdot$ formed in eq 40 would be intercepted as in eq 33 (Scheme IV) to afford ultimately the disubstituted byproduct.[52] The validity of this formulation is reinforced by the observation (see Experimental Section) that the hydridomanganese complex formed from the electroreduction of $Mn(CO)_5NCMe^+$ (II) in the presence of dimethylphenylphosphine is completely substituted; i.e.

$$Mn(CO)_5NCMe^+ + PMe_2Ph \xrightarrow{[+e^-]} HMn(CO)_3(PMe_2Ph)_2 \quad (42)$$

The same hydridomanganese complex is obtained quantitatively from the reduction of the parent $Mn(CO)_6^+$ under similar conditions;[53] i.e.

$$Mn(CO)_6^+ + PMe_2Ph \xrightarrow{[+e^-]} HMn(CO)_3(PMe_2Ph)_2 \quad (43)$$

In both cases, the labile 19-electron and 17-electron radicals are the intermediates responsible for ligand substitution since the carbonylmanganese cations are relatively inert to substitution (compare eq 1 and 2).

Summary and Conclusion

The electroreduction of the carbonylmanganese(I) cation $Mn(CO)_5L^+$ with I (L = CO), II (L = MeCN and py), and III (L = various phosphines (P)) at a potential of ca. −1.4 V vs. SCE requires 1.3 ± 0.2 electrons by galvanostatic coulometry. The examination of the transient electrochemical behavior of the cations by cyclic voltammetry also reveals the presence of a series of irreversible cathodic waves, the peak currents of which correspond to the same electron uptake. Accordingly, the cathodic process is ascribed to a 1-electron reduction of I, II, and III to produce the transient 19-electron radicals $Mn(CO)_5L^\cdot$.

The comparison of the products derived from bulk electrolysis and the intermediates observed during cyclic voltammetry provides a consistent pattern of behavior of the initially formed 19-electron radical $Mn(CO)_5L^\cdot$ involving (a) ligand loss to afford the corresponding 17-electron radicals $Mn(CO)_5^\cdot$ and/or $Mn(CO)_4L^\cdot$ and (b) the hydrogen atom abstraction from the electrolytic medium to lead eventually to the hydridomanganese complexes $HMn(CO)_4P$ and $HMn(CO)_3P_2$. Likewise, the behavior of the 17-electron radicals relates directly to the production of the corresponding anions $Mn(CO)_5^-$ and $Mn(CO)_4L^-$ by a facile reduction at the cathode, which largely precludes the homolytic dimerization to the corresponding dimanganese carbonyls. Instead, the latter are derived by an unusually selective ionic coupling of the anions $Mn(CO)_5^-$ and $Mn(CO)_4L^-$ with the reactant cations $Mn(CO)_5L^+$. The lability of the 17-electron radical accounts for the multiple ligand substitution observed in the hydridomanganese byproduct.

Experimental Section

Materials. The carbonylmanganese(I) cations $Mn(CO)_6^+BF_4^-$,[8] $Mn(CO)_5NCMe^+PF_6^-$,[7] and $Mn(CO)_5py^+BF_4^-$[7] and the phosphine analogues $Mn(CO)_5P^+PF_6^-$ (BF_4^-)[7] were generally prepared as described in the literature. With the phosphine cations, it was found that if $Mn(CO)_5NCMe^+PF_6^-$ was dissolved in acetone together with 1.0–1.3 equiv of phosphine (PPh_3) and the mixture stirred at room temperature with no care exercised to exclude light, a mixture of $Mn(CO)_5PPh_3^+PF_6^-$ and $Mn(CO)_4(PPh_3)_2^+PF_6^-$ was invariably obtained in an ~10:1 mole ratio. Cleaner conversion to the monosubstituted phosphine was obtained if light was rigorously excluded and the reaction mixture stirred for 24 h under an argon atmosphere. Small amounts of the bis(phosphine) cation invariably accompanied $Mn(CO)_5P^+PF_6^-$. Although the contaminant could be separated by successive crystallization, pure $Mn(CO)_5P^+$ salts were also prepared independently by oxidative cleavage of the dimeric $Mn_2(CO)_8P_2$[7] with $NOBF_4$.[9] The physical constants and analytical data of the carbonylmanganese cations are included in Table VI.

The other carbonylmanganese derivatives $Mn(CO)_5^-Na^+$,[10] $Mn(CO)_4PPh_3^-Na^+$,[11] $HMn(CO)_4PPh_3$,[14] $HMn(CO)_3(PPh_3)_2$,[15] and $HMn(CO)_3(PMe_2Ph)_2$[15] were prepared by literature procedures.

All reagents were reagent grade material from commercial sources and used without further purification unless specified. Tetrahydrofuran (Du Pont) was stirred over blue sodium–benzophenone for 24 h, and then the mixture was refluxed for 5 h. This was followed by fractional distillation and storage in Schlenk flasks under argon. Acetonitrile (Fisher) was stirred over $KMnO_4$ for 2 h at room temperature, and the mixture was refluxed for an additional 1 h. After filtration of MnO_2, the clear liquid was treated with diethylenetriamine. Phosphorus pentoxide was added, and then the mixture was refluxed for 5 h. Fractionation under argon afforded pure acetonitrile, which was stored under argon in a Schlenk flask.

Triphenylphosphine (Matheson Coleman and Bell) and tri-*p*-tolylphosphine (M and T) were resublimed prior to use. All of the other phosphines were prepared from either trichlorophosphine (Mallinckrodt),

(50) (a) Kidd, D. R.; Brown, T. L. *J. Am. Chem. Soc.* **1978**, *100*, 4095. (b) Byers, B. H.; Brown, T. L. *J. Am. Chem. Soc.* **1977**, *99*, 2527. (c) Hoffman, N. W.; Brown, T. L. *Inorg. Chem.* **1978**, *17*, 613. (d) Absi-Halabi, M.; Brown, T. L. *J. Am. Chem. Soc.* **1977**, *99*, 2982. (e) Fox, A.; Malito, J.; Poe, A. *J. Chem. Soc., Chem. Commun.* **1981**, 1052. (f) McCullen, S. B.; Walker, H. W.; Brown, T. L. *J. Am. Chem. Soc.* **1982**, *104*, 4007. (g) Shi, A.; Richmond, T. G.; Trogler, W. C.; Basolo, F. *J. Am. Chem. Soc.* **1982**, *104*, 4032.

(51) For a recent summary, see: Herrinton, T. R.; Brown, T. L. *J. Am. Chem. Soc.* **1985**, *107*, 5700. For Mn–Mn bond strength, see: Goodman, J. L.; Peters, K. S.; Vaida, V. *Organometallics* **1986**, *5*, 815.

(52) (a) This formulation requires that the 19-electron radical $Mn(CO)_4P_2^\cdot$ be an intermediate in ligand substitution. See the comments in ref 32. (b) Since the concentration of the 17-electron $Mn(CO)_4P^\cdot$ extant in the bulk solution is low (compare eq 28), the substitution in eq 40 undoubtedly occurs in the diffusion layer owing to high local concentrations of P derived from the fragmentation of the 19-electron $Mn(CO)_5P^\cdot$ in eq 30.

(53) The formation of $HMn(CO)_3P_2$ in significant amounts via Scheme VI and in eq 42 and 43 indicates that ligand substitution in the 17-electron radical is sufficiently facile to compete with reduction (see ref 34).

Table VII. Typical Effect of the Pulse Width on the Current Ratio during the Double-Step Chronoamperometry of Carbonylmanganese Cations[a]

θ, s	$\theta/4$, s	$i_c[Mn(CO)_5P^+]\theta^{1/2}$, $\mu A\ s^{1/2}$	R_2/R_1
1.00	0.25	0.43	2.94
1.50	0.375	0.39	2.99
4.00	1.00	0.42	2.97
6.00	1.50	0.42	2.96

[a] For 5×10^{-3} M $Mn(CO)_5[(p\text{-}MeOPh)_3P]^+PF_6^-$ in THF containing 0.3 M TBAP at 20 °C (see text).

dichlorophenylphosphine (Pressure Chemical), or chlorodiphenylphosphine (Aldrich) with the appropriate Grignard reagent or organolithium reagent.[28] Tetra-*n*-butylammonium perchlorate (TBAP, from G. F. Smith) was recrystallized from ethyl acetate and dried in vacuo. Tetraethylammonium perchlorate (TEAP, from G. F. Smith) was recrystallized from a ternary mixture of absolute ethanol–acetonitrile–ether and dried in vacuo.

Instrumentation and Electrochemical Methods. Infrared spectra were recorded on a Nicolet 10DX FT spectrometer. ^1H NMR spectra were obtained with a JEOL FX-90Q spectrometer, and all chemical shifts are relative to Me_4Si. Cyclic voltammetry was performed on an *iR*-compensated potentiostat[54] driven by a Princeton Applied Research (PAR) Model 175 universal programmer. The high-impedance voltage-follower amplifier was mounted external to the potentiostat to minimize the length of the connection to the reference electrode for low noise pickup. CV curves were either displayed on a Tektronix Model 5115 storage oscilloscope or recorded on a Houston Series 2000 x-y recorder. The aging of the solutions was generally not a problem, and we were able to reproduce the potential–current profiles throughout an experiment. The platinum working electrode was periodically polished with a fine emery cloth. The CV cell was of airtight design with high-vacuum Teflon valves and Viton O-ring seals to allow an inert atmosphere to be maintained without contamination by grease. The working electrode consisted of an adjustable platinum disk embedded in a glass seal to allow periodic polishing without changing the surface area ($\sim$1 mm^2) significantly. The SCE reference electrode and its salt bridge were separated from the catholyte by a sintered-glass frit. The counter electrode consisted of a platinum gauze that was separated from the working electrode by $\sim$3 mm. It was connected to the reference electrode via a 0.1-μF capacitor to aid in the compensation for *iR* drop. Double-step chronoamperometry was carried out in the same electrochemical cell. The PAR programmer was set up to perform a cathodic potential step on the plateau of the reduction wave of $Mn(CO)_5L^+$. The time duration θ was varied typically 2, 4, 6, 8, and 10 s. At the end of θ, the potential was fixed to a value between the anodic waves of $Mn(CO)_5^-$ and $Mn(CO)_4L^-$. The anodic current was recorded at $\theta/4$ to yield the current ratio $R_1 = |i_1(5\theta/4)/i(\theta)|$. In a second run, the same cathodic pulse was performed, but the oxidation pulse was adjusted to a potential beyond that for $Mn(CO)_5^-$ to afford $R_2 = |i_2(5\theta/4)/i(\theta)|$. Note that the cathodic current function $i(\theta) \equiv i_c[Mn(CO)_5L^+]$ and the anodic current functions $i_1(5\theta/4) \equiv i_a[Mn(CO)_4P^-]$ and $i_2(5\theta/4) \equiv i_a([Mn(CO)_4P^-] + [Mn(CO)_5^-])$. The value of the ratio R_2/R_1 was invariant with θ as shown in Table VII. Furthermore, all runs were checked to ensure that the reduction current $i(\theta)$ was constant within the experimental uncertainty. Proceeding from the formulation in eq 30, the ratio relates to the anodic currents and the anion concentration according to

$$\frac{R_2}{R_1} = \frac{i_a([Mn(CO)_5^-] + [Mn(CO)_4P^-])}{i_a[Mn(CO)_4P^-]} \tag{44}$$

or

$$\frac{R_2}{R_1} - 1 = \frac{i_a[Mn(CO)_5^-]}{i_a[Mn(CO)_4P^-]} = r \tag{45}$$

The ratios r (to the extent to which the anodic currents are proportional to the anions formed[55]) yield the relative concentrations of $[Mn(CO)_5^-]$ and $[Mn(CO)_4P^-]$, which are as listed in Table IV. These concentration ratios are also directly related to the ratio of the rate constants k_P/k_{CO} which is plotted in Figure 7. The values of pK_a and the cone angles used in this study are summarized in Table VIII. The derivation of eq 45 requires that r be constant with time, which was verified for all the carbonylmanganese cations (with the exception of $Mn(CO)_5PEt_3^+$). With the latter, $\log r = 0.691\theta - 0.538$ (with a correlation coefficient of 0.991). The discrepancy probably arises from the fast coupling reaction of the newly formed $Mn(CO)_4PEt_3^-$ with its precursor $Mn(CO)_5PEt_3^+$ (compare Table V). Support for this rationalization derives from the use of the extrapolated point for $\log r = -0.538$ at $\theta = 0$, which fits with the correlation in Figure 7.

Table VIII. Donor and Steric Properties of Phosphines

phosphine	pK_a[a]	cone angle, deg[b]	phosphine	pK_a[a]	cone angle, deg[b]
PPh_3	3.04	145	$PhEt_2P$	6.78	136
$(p\text{-}MeOPh)_3P$	5.19	145	Et_3P	8.65	132
$(o\text{-}MeOPh)_3P$	6.17	194	Ph_2MeP	4.65	136
$(p\text{-}Tol)_3P$	4.40	145	$PhMe_2P$	6.25	122
Ph_2EtP	4.91	140			

[a] See ref 28. [b] From ref 41.

Preparative-Scale Electrolysis of Carbonylmanganese Cations. The electroreductions were carried out with a PAR Model 173 potentiostat/galvanostat equipped with either a PAR Model 176 current-to-voltage converter or PAR Model 179 digital coulometer, both of which provided a feedback compensation for ohmic drop between the working and reference electrodes. The voltage-follower amplifier (PAR Model 178) was mounted external to the potentiostat with a minimum length of high-impedance connection to the reference electrode. A 0.1-μF capacitor was connected between the voltage-follower amplifier lead and the counter electrode to ensure low noise pickup. The electrochemical cell was of airless design and allowed a CV electrode to be accommodated to monitor conveniently the solution during the electrolysis. The counter electrode was constructed of a double coil of nichrome wire with a large surface area. The working electrode consisted of a platinum-wire cage wrapped with platinum gauze with a total surface area of $\sim$1.1 cm^3. The electroreductions were generally carried out at a constant current of 3 mA. The time to electrolyze the carbonylmanganese cation completely was compared with the time calculated from Faraday's law to provide values of n in Table I. The end of electrolysis was determined by monitoring the concentration of the carbonylmanganese cation by cyclic voltammetry (vide supra). The latter qualitatively coincided with a significant shift in the potential.

In a typical procedure, a solution of 0.065 g (0.21 mmol) of $Mn(CO)_6^+BF_4^-$ in 26 mL of acetonitrile containing 0.2 M TBAP was electrolyzed with a constant current of 3 mA. The course of electroreduction was followed by taking periodic cyclic voltammograms of the catholyte. The volume of CO evolved was measured by a gas buret. The platinum cathode was blackened. Alternatively, the carbonylmanganese cation $Mn(CO)_5NCMe^+PF_6^-$ (0.21 mmol) was reduced in 26 mL of tetrahydrofuran (THF) containing 0.3 M TBAP. No gas was evolved, and the cathode remained shiny.

The products of electroreduction were identified by a comparison to spectra of authentic samples or reported literature values. Quantification was performed with calibration curves of the IR absorbance vs. concentration of the most intense carbonyl band. The relevant spectral bands for the various carbonylmanganese compounds in THF are as follows (ν_{CO}, cm^{-1}): $Mn(CO)_5^-N(Bu)_4^+$ 1901.7, 1863.7; $Mn_2(CO)_{10}$ 2045.2, 2011.9, 1983.0; $Mn_2(CO)_8(PPh_3)_2$ 1982.2 (vw), 1954.5 (s); $Mn(CO)_4PPh_3^-Na^+$ 1943.4, 1897.6 (br), 1853.1, 1827.3, 1777.0; $HMn(CO)_3(PPh_3)_2$ 1957.0 (br, w), 1916.5 (s); $HMn(CO)_4(PPh_3)$ 2060.0, 1977.3 (sh), 1965.6, 1952.9; $HMn(CO)_5$ 2118.0, 2016.1, 2007.3; $Mn_2(CO)_8[(p\text{-}Tol)_3P]_2$ 1952.9; $HMn(CO)_4[(p\text{-}Tol)_3P]$ 2057.6 (high-energy band only); $Mn_2(CO)_8(Et_2PhP)$ 1946.0; $HMn(CO)_4(Et_2PhP)$ 2057.0 (high-energy band only); $Mn_2(CO_8(Ph_2MeP)_2$ 1952.1; $HMn(CO)_4(Ph_2MeP)$ 2059.4 (high-energy band); $Mn_2(CO)_8[(o\text{-}MeOPh)_3P]_2$ 1946.6; $Mn_2(CO)_8[(p\text{-}MeOPh)_3P]_2$ 1950.0; $HMn(CO)_4(p\text{-}MeOPh_3P)$ 2056.3 (high-energy band only); $Mn_2(CO)_8(Me_2PhP)_2$ 1947.8; $HMn(CO)_4(Me_2PhP)$ 2059.1 (high-energy band only); $Mn_2(CO)_8(Et_3P)_2$ 1944.6; $HMn(CO)_4(Et_3P)$ 2054.4 (high-energy band only); $Mn_2(CO)_8(Ph_2EtP)_2$ 1951.3; $HMn(CO)_4(Ph_2EtP)$ 2059.3 (high-energy band only). The ^1H NMR chemical shifts of the various hydridomanganese compounds in C_6D_6 are as follows (δ (multiplicity) [J(PH), Hz]): $HMn(CO)_4PPh_3$ −6.89 (d) [34.18]; $HMn(CO)_3(PPh_3)_2$ −6.74 (t) [26.85]; $HMn(CO)_3[(p\text{-}MeOPh)_3P]_2$ −6.34 (t) [26.85]; $HMn(CO)_4[(p\text{-}Tol)_3P]$ −6.80 (d) [34.20]; $HMn(CO)_3[(p\text{-}Tol)_3P]_2$ −6.65 (t) [26.86]; $HMn(CO)_4(Ph_2EtP)$ −7.28 (d) [36.52]; $HMn(CO)_3(Ph_2EtP)_2$ −7.52 (t) [31.73]; $HMn(CO)_4(Et_2PhP)$ −7.44 (d) [35.62]; $HMn(CO)_4(Et_3P)$ −7.91 (d) [36.62]; $HMn(CO)_3(Ph_2MeP)_2$ −7.27 (t) [31.74]; $HMn(CO)_4$-

(54) Garreau, D.; Saveant, J. M. *J. Electroanal. Chem. Interfacial Electrochem.* **1972**, *35*, 309; **1974**, *50*, 1.

(55) Provided the anions do not evolve further. That this is not the case is established by the constancy of R_1 and R_2 with θ.

(Ph_2MeP) −7.33 (d) [39.06]; $HMn(CO)_3(PhMe_2P)_2$ −7.62 (t) [34.18]; $HMn(CO)_4(PhMe_2P)$ −7.67 (d) [39.07].

The Mn–Mn dimers were analyzed by quantitative IR spectrophotometry of the principal carbonyl band (ν_{CO}): $Mn_2(CO)_{10}$, 2011.9 cm^{-1}; $Mn_2(CO)_8(PPh_3)_2$, 1954.5 cm^{-1}; $Mn_2(CO)_8(PEt_3)_2$, 1944.6 cm^{-1}; $Mn_2(CO)_8(PMe_2Ph)_2$, 1948.2 cm^{-1}. In every case a calibration curve was linear (correlation coefficient >0.999).

The electroreduction of $Mn(CO)_6^+$ was also carried out in the presence of 20 equiv of PMe_2Ph in acetonitrile containing 0.2 M TBAP, by a procedure similar to that described above. The value of n = 1.0 was obtained with the concomitant evolution of 2.2 equiv of CO. Analysis of the catholyte indicated that a quantitative yield of $HMn(CO)_3(PMe_2Ph)_2$ was formed. When the same reduction was carried out in acetonitrile-d_3, only $HMn(CO)_3(PMe_2Ph)_2$ was observed with no deuterium incorporation. Similarly, the electroreduction of $Mn(CO)_5NCMe^+$ with 10 equiv of PMe_2Ph was carried out in THF containing 0.3 M TBAP. The value of n = 0.85 reflected competition from the thermal substitution of PMe_2Ph for MeCN. Nonetheless, the major product was $HMn(CO)_3(PMe_2Ph)_2$ contaminated with a small amount of $Mn_2(CO)_8(PMe_2Ph)_2$ and an unknown species with ν_{CO} = 1987.1 cm^{-1}.

Heterolytic Coupling of Carbonylmanganese Anions with Cations. The cross-coupling of carbonylmanganese cations and anions was carried out under the conditions of the electroreduction. In a typical example, a 3 × 10^{-3} M solution of $Mn(CO)_5NCMe^+PF_6^-$ was made up in THF containing 0.3 M TBAP under an argon atmosphere. A separate stock solution of $Mn(CO)_5^-Na^+$ was made up, and an aliquot containing 1 equiv of anion was added to the solution of the cation with the aid of a hypodermic syringe. The course of the coupling was followed by periodically extracting a sample for IR analysis. The reactions between $Mn(CO)_5^-Na^+$ and either $Mn(CO)_5NCMe^+$ or $Mn(CO)_5py^+$ were complete within the time the first IR spectrum could be measured. They yielded $Mn_2(CO)_{10}$ quantitatively. A similar rapid reaction of $Mn(CO)_4PPh_3^-Na^+$ with $Mn(CO)_5PPh_3^+$ afforded quantitative yields of $Mn_2(CO)_8(PPh_3)_2$ by IR analysis. In contrast, the reaction of $Mn(CO)_5PEt_3^+$ with $Mn(CO)_5^-Na^+$ was too slow to observe within a 10-h period. The reaction of $Mn(CO)_5(o\text{-}MeOC_6H_4)_3P^+$ with $Mn(CO)_5^-Na^+$ afforded ~15% of $Mn_2(CO)_{10}$ after 30 min and was complete after 4 h. The mixture of $Mn(CO)_6^+PF_6^-$ and $Mn(CO)_5^-Na^+$ in acetonitrile containing 0.2 M TBAP did not show any significant reaction after 30 min. After 24 h no starting materials were apparent, being replaced by new IR bands of $Mn_2(CO)_{10}$ and an unidentified species with ν_{CO} = 2064.3 cm^{-1}.

Cyclic Voltammetry of Carbonylmanganese Cations. In a typical procedure, a thoroughly dried, argon-filled CV cell (at 150 °C followed by cooling in vacuo) was charged with 0.0114 g (3 × 10^{-5} mol) of $Mn(CO)_5NCMe^+PF_6^-$ and an anaerobic solution of 1.03 g (3 × 10^{-3} mol) of TBAP in 10 mL of THF was added to fill both compartments of the working electrode (6 mL) and the reference electrode (4 mL). Cyclic voltammograms were obtained at scan rates varying from 100 mV s^{-1} to 100 V s^{-1}. The reproducibility of the current–potential profiles was excellent, with no evidence for electrode pollution over a period of hours. All the CV waves observed in this study were diffusive, and we found no evidence of adsorbed species on the working electrode.[56] The peak potentials and cathodic currents were calibrated by comparison with those of a ferrocene standard.[16]

Acknowledgment. We thank B. A. Narayanan for instigating this research and for many helpful discussions and the National Science Foundation and Robert A. Welch Foundation for financial support.

Registry No. $Mn(CO)_6^+$, 21331-06-6; $Mn(CO)_5NCMe^+$, 27674-37-9; $Mn(CO)_5py^+$, 54039-53-1; $Mn(CO)_5PPh_3^+$, 54039-45-1; $Mn(CO)_5(p\text{-}MeOPh)_3P^+$, 104350-76-7; $Mn(CO)_5(o\text{-}MeOPh)_3P^+$, 104350-77-8; $Mn(CO)_5\text{-}p\text{-}Tol_3P^+$, 54039-58-6; $Mn(CO)_5Et_2PhP^+$, 71465-42-4; $Mn(CO)_5EtPh_2P^+$, 71465-46-8; $Mn(CO)_5Et_3P^+$, 68166-16-5; $Mn(CO)_5MePh_2P^+$, 71465-44-6; $Mn(CO)_5(PhMe_2P)^+$, 54039-47-3; $Mn(CO)_5^-$, 14971-26-7; $Mn_2(CO)_{10}$, 10170-69-1; $Mn_2(CO)_8(PPh_3)_2$, 10170-70-4; $Mn_2(CO)_8[(p\text{-}MeOPh)_3P]_2$, 15662-85-8; $Mn_2(CO)_8[(o\text{-}MeOPh)_3P]_2$, 104350-78-9; $Mn_2(CO)_8[p\text{-}Tol_3P]_2$, 63588-37-4; $Mn_2(CO)_8[Et_2PhP]_2$, 15444-75-4; $Mn_2(CO)_8[EtPh_2P]_2$, 15444-76-5; $Mn_2(CO)_8[Et_3P]_2$, 15529-60-9; $Mn_2(CO)_8[MePh_2P]_2$, 63393-52-2; $Mn_2(CO)_8[Me_2PhP]_2$, 55029-78-2; $HMn(CO)_4PPh_3$, 16925-29-4; $HMn(CO)_4(p\text{-}MeOPh)_3P$, 104419-61-6; $HMn(CO)_4\text{-}p\text{-}Tol_3P$, 104419-62-7; $HMn(CO)_4Et_2PhP$, 104350-79-0; $HMn(CO)_4EtPh_2P$, 92816-72-3; $HMn(CO)_4Et_3P$, 68199-71-3; $HMn(CO)_4MePh_2P$, 104350-80-3; $HMn(CO)_4Me_2PhP$, 104419-63-8; $HMn(CO)_3[PPh_3]_2$, 16972-17-1; $HMn(CO)_3[(p\text{-}MeOPh)_3P]_2$, 104350-81-4; $HMn(CO)_3[p\text{-}Tol_3P]_2$, 80512-13-6; $HMn(CO)_3[Et_2PhP]_2$, 104350-82-5; $HMn(CO)_3[MePh_2P]_2$, 42965-72-0; $HMn(CO)_3[Me_2PhP]_2$, 86708-28-3; $Mn(CO)_6^\bullet$, 104350-83-6; $Mn(CO)_5NCMe^\bullet$, 104350-84-7; $Mn(CO)_5py^\bullet$, 104350-85-8; $Mn(CO)_5PPh_3^\bullet$, 104350-86-9; $Mn(CO)_5P(p\text{-}MeOPh)_3^\bullet$, 104350-87-0; $Mn(CO)_5P(o\text{-}MeOPh)_3^\bullet$, 104350-88-1; $Mn(CO)_5P(p\text{-}Tol)_3^\bullet$, 104350-89-2; $Mn(CO)_5PEt_2Ph^\bullet$, 104350-90-5; $Mn(CO)_5PEtPh_2^\bullet$, 104350-91-6; $Mn(CO)_5PEt_3^\bullet$, 104350-92-7; $Mn(CO)_5PMePh_2^\bullet$, 104350-93-8; $Mn(CO)_5PMe_2Ph^\bullet$, 104350-94-9; $Mn(CO)_6^+BF_4^-$, 15557-71-8; $Mn(CO)_5py^+BF_4^-$, 96412-38-3; $Mn(CO)_5NCMe^+PF_6^-$, 37504-44-2; $Mn(CO)_5PPh_3^+PF_6^-$, 54039-57-5; $Mn(CO)_5[(p\text{-}MeOPh)_3P]^+PF_6^-$, 104350-95-0; $Mn(CO)_5[(o\text{-}MeOPh)_3P]^+PF_6^-$, 104350-96-1; $Mn(CO)_5[(p\text{-}Tol)_3P]^+PF_6^-$, 54039-59-7; $Mn(CO)_5(Ph_2EtP)^+PF_6^-$, 104350-97-2; $Mn(CO)_5(PhEt_2P)^+PF_6^-$, 104350-98-3; $Mn(CO)_5Et_3P^+PF_6^-$, 68166-17-6; $Mn(CO)_5(Ph_2MeP)^+PF_6^-$, 104350-99-4; $Mn(CO)_5(PhMe_2P)^+PF_6^-$, 54039-52-0; $Mn(CO)_5PPh_3^+BF_4^-$, 54039-46-2; $Mn(CO)_5^-Na^+$, 13859-41-1; $Mn(CO)_4PPh_3^-Na^+$, 19457-74-0; $Mn(CO)_4PPh_3^-$, 53418-18-1; $Mn(CO)_4P(p\text{-}MeOPh)_3^-$, 104351-00-0; $Mn(CO)_4P(p\text{-}Tol)_3^-$, 104351-01-1; $Mn(CO)_4PEtPh_2^-$, 104351-02-2; $Mn(CO)_4PEt_2Ph^-$, 104351-03-3; $Mn(CO)_4PEt_3^-$, 104351-04-4; $Mn(CO)_4PMePh_2^-$, 62390-50-5; $Mn(CO)_4PMe_2Ph^-$, 104351-05-5.

(56) The characteristic current responses for adsorbed, electroactive species is described by: Kissinger, P. T.; Heineman, W. R. *Laboratory Techniques in Electroanalytical Chemistry*; Dekker: New York, 1984; p 46ff.